JPhys Photonics

PAPER • OPEN ACCESS

Photoelectron spectroscopy of large water clusters ionized by an XUV comb

Recent citations

- Below Band Gap Formation of Solvated Electrons in Neutral Water Clusters?
Loren Ban *et al*

To cite this article: Andrea Trabattoni *et al* 2020 *J. Phys. Photonics* **2** 035007

View the article online for updates and enhancements.

This content was downloaded from IP address 130.183.90.175 on 04/11/2020 at 09:34

Journal of Physics: Photonics

OPEN ACCESS

RECEIVED
20 February 2020

REVISED
21 April 2020

ACCEPTED FOR PUBLICATION
13 May 2020

PUBLISHED
26 June 2020

Original content from this work may be used under the terms of the Creative Commons Attribution 4.0 licence. Any further distribution of this work must maintain attribution to the author(s) and the title of the work, journal citation and DOI.

PAPER

Photoelectron spectroscopy of large water clusters ionized by an XUV comb

Andrea Trabattoni[1,10], Lorenzo Colaizzi[1,2,10], Loren Ban[3,10], Vincent Wanie[1,4], Krishna Saraswathula[1], Erik P Månsson[1], Philipp Rupp[5,6], Qingcao Liu[5,6], Lennart Seiffert[7], Elisabeth A Herzig[7], Andrea Cartella[1,8], Bruce L Yoder[3], François Légaré[4], Matthias F Kling[5,6], Thomas Fennel[7], Ruth Signorell[3] and Francesca Calegari[1,2,8,9]

[1] Center for Free-Electron Laser Science, DESY, Notkestr. 85, 22607, Hamburg, Germany
[2] Physics Department, University of Hamburg, Luruper Chaussee 149, 22761, Hamburg, Germany
[3] Department of Chemistry and Applied Biosciences, Laboratory of Physical Chemistry, ETH Zürich, Vladimir-Prelog-Weg 2, 8093, Zürich, Switzerland
[4] Centre Énergie Matériaux Télécommunications, Institut National de la Recherche Scientifique, 1650 Blvd. Lionel-Boulet, J3X 1S2, Varennes, Canada
[5] Max Planck Institute of Quantum Optics, Hans-Kopfermann-straße 1, 85748, Garching, Germany
[6] Department of Physics, Ludwig-Maximilians-Universität München, Am Coulombwall 1, 85748, Garching, Germany
[7] Institute of Physics, University of Rostock, Albert-Einstein-Str. 23, 18059, Rostock, Germany
[8] The Hamburg Centre for Ultrafast Imaging, Universität Hamburg, 149 Luruper Chaussee, 22761, Hamburg, Germany
[9] Institute for Photonics and Nanotechnologies CNR-IFN, P.za Leonardo da Vinci 32, 20133, Milano, Italy

E-mail: andrea.trabattoni@desy.de

Keywords: photoelectron spectroscopy, water clusters, extreme-ultraviolet ionisation

Abstract

Detailed knowledge about photo-induced electron dynamics in water is key to the understanding of several biological and chemical mechanisms, in particular for those resulting from ionizing radiation. Here we report a method to obtain photoelectron spectra from neutral water clusters following ionization by an extreme-ultraviolet (XUV) attosecond pulse train, representing a first step towards a time-resolved analysis. Typically, a large background signal in the experiment arises from water monomers and carrier gas used in the cluster source. We report a protocol to quantify this background in order to eliminate it from the experimental spectra. We disentangle the accumulated XUV photoionization signal into contributions from the background species and the photoelectron spectra from the clusters. This proof-of-principle study demonstrates feasibility of background free photoelectron spectra of neutral water clusters ionized by XUV combs and paves the way for the detailed time-resolved analysis of the underlying dynamics.

1. Introduction

A detailed understanding of electron scattering properties in water is crucial to modeling and controlling many processes occurring in nature, ranging from atmospheric chemistry to radiation biology [1–3]. When highly energetic radiation interacts with biological tissue, for example, an ionization track leads to the formation of many intermediate species, eventually breaking down the tissue into smaller products. During this process, low-energy electrons (kinetic energies between 10 and 50 eV) have been shown to play a central role in DNA damage [4–6]. As a bottom-up approach to understand the dynamics of such complex systems, the investigation of electron scattering and transport properties in water is essential [7–11]. Scattering cross sections for liquid water have been retrieved in the sub-excitation range [9, 12]. However, the only available data on electron scattering cross sections in the 10–50 eV energy range is for amorphous ice [13]. Recently, electron scattering in large neutral water clusters $(H_2O)_n$ was investigated and compared to condensed-phase data [14, 15].

[10] These authors contributed equally to this work.

© 2020 The Author(s). Published by IOP Publishing Ltd

Although the above-mentioned studies shed light on low-energy electron scattering in water, mainly in terms of scattering cross sections and channel-resolved energy losses, no time-resolved studies of electron scattering in clusters have been reported to date. It is known that low-energy electrons propagating through biological tissue induce non-thermal reactions on ultrafast time scales, typically in the femtosecond regime. However, the timing of the elementary step in this chain of events, i.e. the scattering time of the electrons in the aqueous medium, has so far not been measured. In this context, time-resolved spectroscopy with high temporal resolution may provide new insight into the ultrafast electron dynamics occurring in hydrated molecules.

The advent of attosecond technology [16] allowed for the investigation of electron dynamics in matter with unprecedented temporal resolution. Building on the seminal results obtained in atoms and small molecules [17–19], attosecond extreme-ultraviolet (XUV) pulses have recently been used to elucidate charge dynamics in more complex systems [20, 21]. In this context, a time-resolved study of electron transport properties in large dielectric nanoparticles was performed [22, 23], and an inelastic scattering time of around 400 as was measured for photoelectron energies between 20 and 30 eV. This result proved that attosecond spectroscopy can be applied to larger samples, bringing the field one step closer to investigation of electron scattering in water with attosecond resolution.

Interfacing attosecond spectroscopy setups and bulk liquid water samples is technologically very challenging. First of all, attosecond laser pulses need to propagate in an ultra-high vacuum, ultra-low optical-dispersion environment, which is difficult to maintain in the presence of liquid water. Moreover, the detection of few-eV electrons generated in liquid samples presents several technical challenges of its own [24]. However, the above-mentioned limitations can be partially circumvented by the employment of molecular sources producing large water clusters in the gas-phase, while providing at the same time an interesting prototype target with specific physical properties that reflect the intermediate position between the gas and liquid phase. Furthermore, electron scattering cross sections are available for neutral water clusters [14].

In this work we report photoelectron spectra of water clusters containing about 100 water molecules ionized by an extreme-ultraviolet (XUV) comb with photon energies between 20 eV and 50 eV.

We focus here on the analysis of the photoelectron spectra, aiming at the extraction of a water cluster signal from those of other species present in the interaction region, in particular water monomers and carrier gas. We show that this can be achieved by performing multiple measurements under different source conditions. By combining these measurements with simulated photoelectron spectra, we disentangle the contributions from the three species of interest: water clusters, water monomers and the carrier gas. This analysis paves the way for the interpretation of attosecond time-resolved photoelectron spectra of water clusters ionized by XUV combs.

2. Experiment

A Ti:Sapphire laser system (Femtopower by Spectra Physics) provided linearly-polarized laser pulses centered at 780 nm, with a temporal width of 20 fs and a pulse energy of 2 mJ. The laser pulses were focused in a pulsed gas jet to drive high-harmonic generation (HHG) in argon [25]. The HHG beam propagated through a thin Al foil (100-nm thickness) that is used to remove the 780-nm driving field. The transmitted HHG signal was focused onto the interaction region with the cluster beam through a grazing-incidence gold-coated toroidal mirror, and its spectrum was measured by an XUV spectrometer installed downstream from the interaction region. The measured XUV spectrum is shown in figure 1(a). It consists of a comb of odd harmonics of the fundamental frequency in the energy range between 20 and 50 eV, i.e. between the 13th and 31st order harmonics.

Water clusters were produced by expanding water vapor through a pulsed Even-Lavie (EL) valve [26] into vacuum, similarly to previous studies [14, 15]. The temperature of the sample reservoir filled with liquid water was set to 383 K. To avoid condensation in the nozzle, the EL valve was held at 388 K. A mixture of water vapor with helium (He) carrier gas at a pressure of ~12 bar was expanded into the interaction region. These conditions resulted in clusters containing about 100 water molecules. This estimate is based on previous Na-doping measurements performed at ETH Zürich [14] and a simulated cluster photoelectron spectrum (see below). Time-of-flight mass spectra and photoelectron velocity map images of water clusters ionized by the XUV harmonic comb were recorded with a velocity map imaging [27] (VMI) spectrometer in a perpendicular extraction configuration [28].

In figure 1(b) we report the measured photoelectron momentum distribution following ionization of the water clusters by the XUV comb. The distribution is integrated over 30 000 laser shots, fully symmetrized along both the x and y axes, normalized to the innermost ring, and plotted on a log scale.

We note that, due to the typical operation of the cluster source explained above, the XUV comb can efficiently generate photoelectrons from all the species that are present in the interaction region, i.e. not only

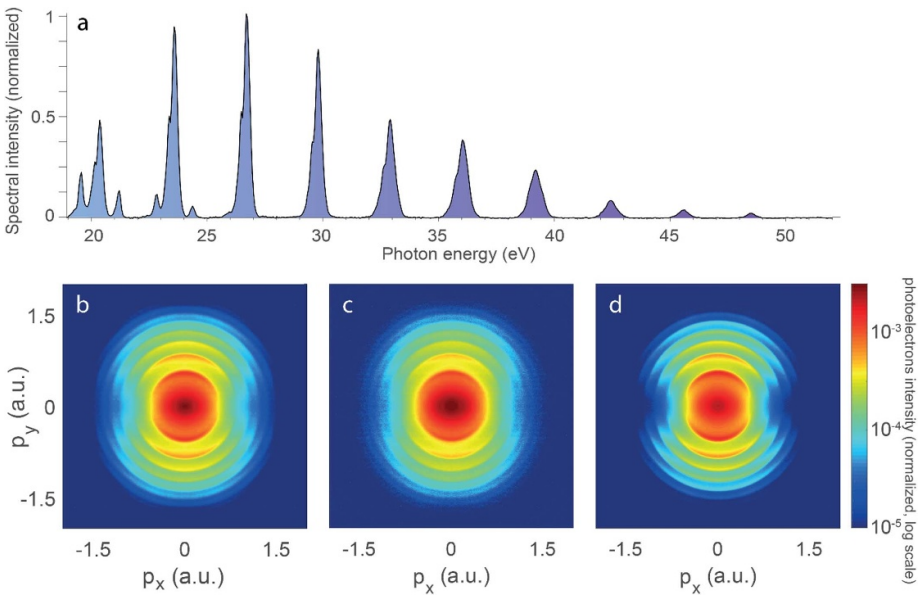

Figure 1. (a): High-harmonic spectrum generated in argon. The satellite peaks below 25 eV originate from higher order diffraction introduced by the grating. b,c,d: 2D Projections of the angle-resolved photoelectron momentum distributions (in atomic units): clusters (b); He/water monomer mixture (c); pure He (d). The images in b,c,d were fully symmetrized along both the x and y axes, normalized to the innermost ring and shown on a logarithmic color scale. The electric field is linearly polarized along the y-axis.

the water clusters under study but also (gas-phase) water monomers and He atoms. In fact, due to their abundance, water monomers and He atoms may represent the dominant contribution to the photoelectron spectrum of figure 1(b) and act as a relatively large background in the experiment. The main goal of this work is to establish a robust analysis procedure that allows for the removal of such a background.

In order to evaluate—and eliminate—contributions of He and water monomers to the spectra and extract a clean photoelectron signal of water clusters, the source was operated under two additional conditions. First, the XUV was synchronized to interact with the rising edge of the temporal profile of the cluster beam pulse, for which a low-density He/water monomer mixture (no clusters) is obtained. Second, a measurement with pure He target was performed. The absence of clusters or water monomer, respectively, was confirmed by mass spectrometry measurements. The resulting photoelectron momentum distributions are shown in figures 1(c) and (d), respectively. The images are individually normalized to the signal of the innermost ring in each image. Before normalization, the ratio of signals for the innermost ring in cluster (figure 1(b)), monomer (figure 1(c)) and helium (figure 1(d)) images is 1:0.25:0.9, as expected from different source conditions employed. Besides the mentioned difference in signal levels, cluster and monomer distributions (figures 1(b),(c)) do not show appreciable differences.

Furthermore, the water monomer photoelectron distribution (figure 1(c)) cannot be directly used as a background to be subtracted from the cluster distribution (figure 1(b)), since the relative abundance of He and water monomers is not the same in different temporal slices of the molecular beam. For this reason, we analyze each distribution from figure 1 separately. We demonstrate that a clear photoelectron signal from clusters can be identified by fitting the simulated XUV photoelectron spectra to the experiment.

In the following we will use the term 'cluster spectrum'—if not specified otherwise—to refer to the first target condition described above, i.e. the mixture of He, water monomer and water clusters. We will use 'He' for a pure helium condition and 'monomer' to refer to the mixture containing helium and water monomers.

3. Analysis and discussion

As a first step, to have a more accurate picture of the photoelectron distributions produced for the three target conditions described above, the full three-dimensional momentum spheres were retrieved by Abel inversion of the 2D projected data of figures 1(b)–(d) on a basis of Legendre polynomials, using the BASEX method [29].Then, the corresponding center-slices of the reconstructed photoelectron distributions were angularly integrated, and the resulting curves were plotted in figure 2(a) as a function of the photoelectron energy for He (green solid line), He/monomer (blue solid line) and clusters (red solid line). In the same figure, the photoelectron energies expected for ionization of He ($I_p = 24.58$ eV) by the XUV comb are given (green dashed vertical lines). The three spectra show an exponentially decaying background signal which we

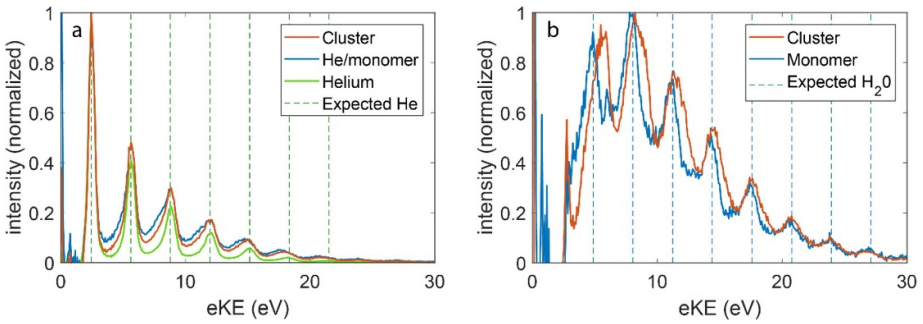

Figure 2. (a): Photoelectron kinetic energy (eKE) spectra obtained by angularly integrating the inverted photoelectron spectra for the three different target conditions, i.e. for clusters (red solid line), He/monomer (blue solid line) and He (green solid line); the spectra were normalized to the first photoelectron peak, after subtracting the baseline; the green dashed lines show the photoelectron energies expected for ionization of He ($I_p = 24.58$ eV) by the XUV comb. (b): Blue and red curves from panel (a) after the subtraction of He, normalized to the maximum signal; the blue dashed lines show the photoelectron energies expected for ionization from the highest occupied molecular orbital of water monomer ($I_p = 12.62$ eV) by our XUV comb.

expect to originate from scattered electrons generated in the long ionization volume defined by the focused XUV pulses. In the following analysis, such background was fitted with a combination of a Gaussian and an exponential function and subtracted from the measured spectra (figure 2(a)). In the cluster spectrum, we note that a minor contribution from secondary electrons is plausible.

We note that the dominant photoelectron peaks match the dashed lines not only in the He spectrum but also in the He/monomer and cluster spectra. This is a clear signature of the predominant contribution of He for all three target conditions.

This was further confirmed by mass spectrometry measurements. The relative abundance of ionized He in He/monomer and cluster conditions was found to be two orders of magnitude higher than the ionized water species. Even without knowing the relative abundance of helium in the different images, it is still possible to extract an experimental ratio from the data, as there is one ring in the image that is produced almost entirely of photoelectrons emitted from He. Since the ionization potential of water is much lower than that of He, only the higher-binding-energy bands of water may contribute to the spectrum at energies <5 eV. Thus, the lowest energy photoelectron peak (at ~2.5 eV) is dominated by helium photoelectrons. The ratio between the intensity of this peak in the different spectra represent therefore the relative abundance of ionized He in clusters and He/monomer spectra. The He background can then be rescaled and removed from the cluster and the monomer spectra.

In figure 2(b) we report the result of the subtraction, indicating the photoelectron energies expected for ionization from the highest occupied molecular orbital of a water monomer ($I_p = 12.62$ eV) by the XUV comb (blue dashed vertical lines). The two spectra were normalized to their maximum value. As a consequence of the subtraction, the spectrum originally measured for the He/monomer case is expected to show a clean signal from the water monomer. Indeed, the peaks of the blue curve match the blue dashed lines. For clusters, instead, the subtracted spectrum (red solid line) consists now of photoelectrons produced by a mixture of clusters and monomers. This is evident in the shoulder shifted towards higher kinetic energies: a clear signature of the cluster contribution, for which the ionization potential is about 0.8 eV lower than that of the monomer [14, 30]. We note that the subtracted spectra show background subtraction artefacts at very low energies (<5 eV). They may originate from a combination of imperfect subtraction of the diffuse low-energy feature and, consequently, imperfect rescaling based on the first photoelectron peak. At energies where photoelectrons from water contribute to the spectra significantly (>5 eV), the subtracted data demonstrates that a significant quantity of photoelectrons was produced from clusters.

We compare the experiment to simulated photoelectron spectra generated by the corresponding XUV light. The simulated photoelectron spectra were obtained by accounting for photoionization of He, water monomers and water clusters by each of the harmonics present in the XUV comb, including the information on XUV spectral intensity and absolute ionization cross sections [31, 32]. The He single harmonic photoelectron spectrum was approximated by a Gaussian function, while the literature-reported water monomer and cluster electron binding energy (eBE) spectra were used [33]. Further details on the simulation can be found in appendix A.

In a first step, we simulated the pure He photoelectron spectrum (green dots, figure 3(a)). By fitting the simulation to the experimental background-subtracted (exponential background) spectrum, we were able to determine relative XUV spectral intensities and the intrinsic resolution of our spectrometer. Due to the large ionization volume defined by the focused XUV light, and electron trajectories far off-center experiencing

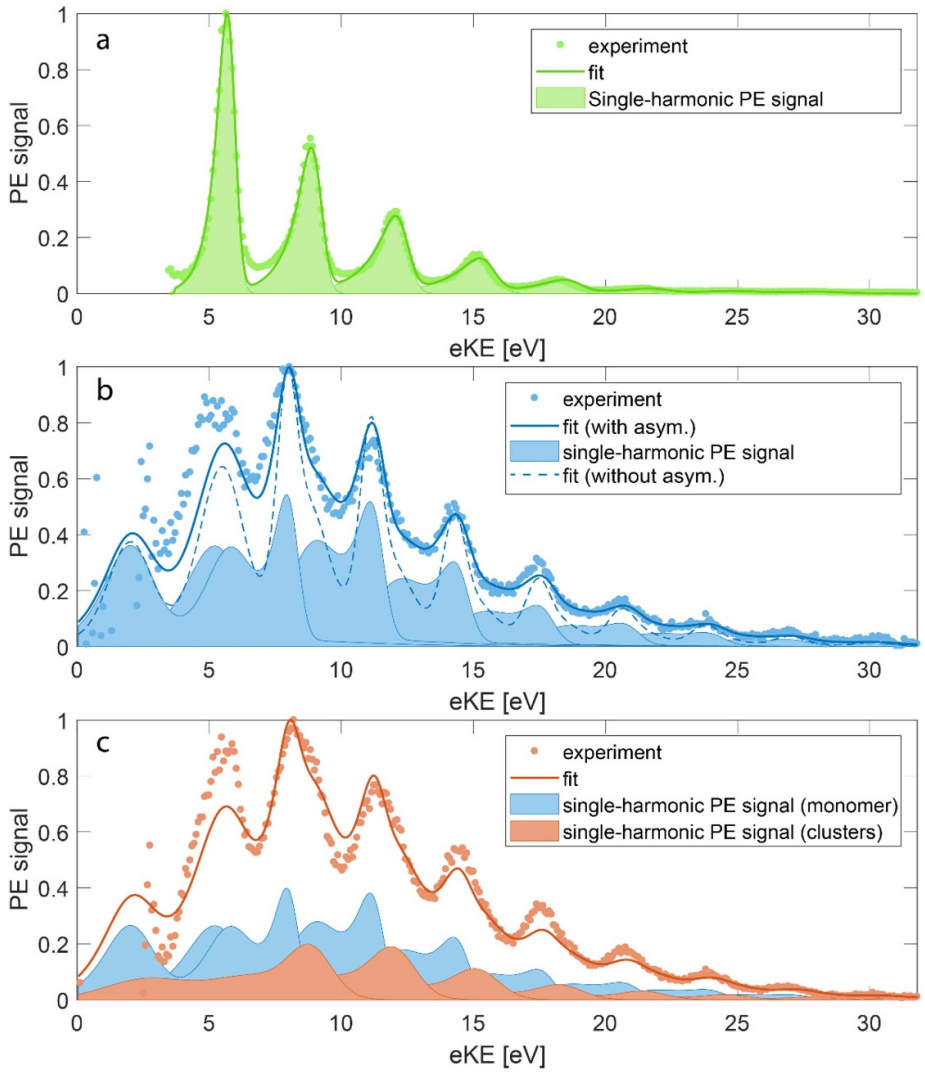

Figure 3. Comparison between experimental spectra and simulations. (a) He spectrum (after subtracting the baseline) is shown in dots. The solid line shows the fit of the overall spectrum, i.e. the sum of the ionization spectra (indicated by green areas) produced by each harmonic where the width, amplitude and asymmetry are fit parameters. The same comparison is reported in (b) for water monomer, where the dashed line represents a fit with same parameters, but without including asymmetric peaks correction and in c) for monomer/cluster mixture.

stronger VMI-lensing, the peaks show an asymmetric shape with a tail extending towards lower electron kinetic energy (eKE). These asymmetries were accounted for by using an exponentially modified Gaussian line shape, characterized by a single asymmetry parameter [34]. Both the linewidth and the asymmetry parameter were assumed to be linearly dependent on the kinetic energy. The resulting simulated spectrum is shown as a solid line in figure 3(a), with individual photoelectron bands shown as shaded areas. The relative XUV spectral intensity agrees with the experimental spectrum (figure 1(a)) within the uncertainties given by the XUV and VMI spectrometers. The linewidths range from 0.2–0.5 eV (full width at half maximum) in going from 2.5 eV to 20 eV kinetic energy.

In a second step, the isolated water monomer spectrum (blue dots, figure 3(b)) was simulated. The XUV spectrum, linewidths and asymmetries obtained in the previous step were held constant. The eBE spectrum of water monomer recorded at photon energy of 22 eV [33] was adapted to include the determined linewidths and peak asymmetries. The solid line in figure 3(b) shows the spectrum resulting from the sum of the individual harmonic components (shown as blue areas in figure 3(b)). To illustrate the importance of correctly accounting for the intrinsic VMI spectrometer peak shapes, a simulated spectrum assuming symmetric line shapes is shown as dashed blue line in figure 3(b).

Finally, we concentrate on the cluster spectrum (red dots, figure 3(c)). The monomer contribution was simulated in the same manner as in the previous step and the line shape parameters kept at values determined in the first step. To account for condensation effects on the cluster photoionization cross section, water monomer data [32] was assumed to scale with an average cluster size. A cluster eBE spectrum was

approximated using a literature spectrum reported for a cluster of 20 molecules ionized with 22 eV light [33]. The relative band intensities in this spectrum are expected to well represent cluster size regime investigated in this study, as well as the photon energies employed for photoionization. Due to the broad nature of the cluster photoelectron bands, no asymmetry was included for the cluster spectrum. A two-parameter fit to the experimental spectrum was performed and the resulting spectrum is shown as solid line in figure 3(c). The first parameter includes a factor allowing for a band shift of 0.8–1.3 eV towards higher eKE (with respect to the monomer), introduced to account for a cluster-size dependent shift in binding energies [14, 30, 35]. The retrieved value of ~0.8 eV is consistent with clusters containing ~100 water molecules [14]. The second parameter yields a ratio of photoelectrons originating from monomers to clusters of 2:1. The two above-mentioned retrieved values represent the main outcome of our analysis and demonstrate that a clear signature of large water clusters can be extracted from experimental spectra.

4. Conclusions

In this work we reported a photoelectron spectroscopy experiment on neutral water clusters ionized by a high harmonic comb in the XUV. We demonstrate that a significant quantity of photoelectrons ejected from neutral water clusters was measured, albeit together with a large background from He and water monomers. We showed that the signature of cluster photoelectrons can be identified in the spectrum by simulating the photoionization of the species present in the interaction region and using the numerical results to fit the experimental data. This allowed us to produce the portion of the experimental spectrum which can be assigned to clusters. This analysis represents an important ingredient for the interpretation of photoelectron spectroscopy experiments on neutral water clusters ionized by an attosecond pulse train. In particular, our result paves the way for the analysis of time-resolved XUV spectroscopy on clusters, such as reconstruction of attosecond beating by interference of two-photon transitions (RABBITT) [36, 37].

Acknowledgments

This work is supported by the DFG-Sonderforschungsbereich 925 'Light-induced dynamics and control of correlated quantum systems' (Project No. A7) and by the Cluster of Excellence 'CUI: Advanced Imaging of Matter' of the Deutsche Forschungsgemeinschaft (DFG)—EXC 2056—project ID 390715994. R S acknowledges funding from the European Union's Horizon 2020 research and innovation program from the European Research Council under the Grant No. 786636, and the research was supported by the NCCR MUST, funded by the Swiss National Science Foundation (SNSF), through ETH-FAST, and through SNSF project No. 200020_172472. R S is also a grateful recipient of a Humboldt Research Prize from the Alexander von Humboldt Foundation and a Mildred Dresselhaus Guestprofessorship from the Centre for Ultrafast Imaging in Hamburg. F C acknowledges support from the European Research Council under the ERC-2014-StG STARLIGHT (Grant No. 637756). V W acknowledges support from the Vanier Canada Graduate Scholarship (CGS) program. P R, Q L, L S, T F, and M F K acknowledge support by the German Research Foundation via SPP1840. T F acknowledges further financial support by the German Research Foundation via the Heisenberg Programme (ID: 398382624). P R, Q L, and M F K are grateful for support by the Max Planck Society through the MP Fellow program.

Appendix A. Simulation and fitting of XUV photoelectron spectra

To model photoelectron spectra produced by XUV-comb ionizing our water-containing molecular beam, we describe the photoelectron signal in terms of spectral components corresponding to each species present in the ionization volume ionized by each of the harmonics

$$\mathrm{PES}\left(eKE\right) = \sum_{k} I_k \sum_{i} A_i \sigma_i \left(k \cdot h\nu\right) \mathrm{PES}_i^k \left(k \cdot h\nu - eBE\right),$$

where I_k is the relative intensity of a harmonic with order k and $h\nu$ is the fundamental photon energy. The relative abundance of each species (i) present in the interaction volume is given by the parameter A_i. Energy dependent photoionization cross sections (σ_i) of helium and water monomer are taken from the literature [31, 32] and we assume that $\sigma_{cluster} = n\sigma_{monomer}$, where n is the average cluster size. The corresponding photoelectron spectra (PES_i^k) are calculated from the photon energy ($k \cdot h\nu$) and the photoelectron binding energy (eBE) spectra.

The PES of helium is represented by an exponentially modified Gaussian function [34]

$$\mathrm{PES}^{k}_{He}\left(eKE\right) = \frac{w}{\alpha}\sqrt{\frac{\pi}{2}}\exp\left[\frac{1}{2}\left(\frac{w}{\alpha}\right)^{2} - \frac{eKE - eKE_0}{\alpha}\right]\left\{1 - \mathrm{erf}\left[\frac{1}{\sqrt{2}}\left(\frac{w}{\alpha} - \frac{eKE - eKE_0}{w}\right)\right]\right\},$$

where w is the peak width and α is the asymmetry parameter. The asymmetric shape towards lower kinetic energies originates from the long ionization volume (Rayleigh length) defined by the focused XUV light, and electron trajectories far off-center experiencing stronger VMI-lensing. The importance of correctly accounting for the asymmetric shape is highlighted in figure 3(b) by comparing the monomer simulation with (full line) and without (dashed line) the asymmetry. Both w and α are assumed to linearly depend on electron kinetic energy. The parameter eKE_0 is determined from the photon energy of harmonic k and the ionization potential of helium so that the center of the band lies at $eKE_0 = k \cdot h\nu - I_\mathrm{P}$.

The *eBE* spectra of water monomer and clusters ($n = 20$) are taken from the literature [33]. The monomer spectrum is described by a sum of 4 Gaussian functions representing photoionization from the $1b_1$, $3a_1$ and $1b_2$ orbitals and afterwards modified to include the determined spectrometer linewidths and peak asymmetries by replacing Gaussian functions by the exponentially modified Gaussian functions. For clusters, no asymmetry is included due to the broad nature of the cluster photoelectron bands. To account for condensation effects on the cluster *eBE* spectrum, we included a size-dependent shift (ΔeBE) [14, 30] so that

$$\mathrm{PES}^{k}_{cluster}\left(eKE\right) = \mathrm{PES}^{k}_{cluster}\left(k \cdot h\nu - eBE + \Delta eBE\right).$$

ORCID iDs

Andrea Trabattoni https://orcid.org/0000-0002-0187-9075
Loren Ban https://orcid.org/0000-0002-9312-2984
Erik P Månsson https://orcid.org/0000-0003-3567-2985
Qingcao Liu https://orcid.org/0000-0002-3691-7369
Lennart Seiffert https://orcid.org/0000-0002-2389-5295
Matthias F Kling https://orcid.org/0000-0002-1710-0775
Thomas Fennel https://orcid.org/0000-0002-4149-5164
Francesca Calegari https://orcid.org/0000-0003-3234-7298

References

[1] Sanche L 2009 Beyond radical thinking *Nature* **461** 358–9
[2] Lu Q B and Sanche L 2001 Effects of cosmic rays on atmospheric chlorofluorocarbon dissociation and ozone depletion *Phys. Rev. Lett.* **87** 078501
[3] Alizadeh E and Sanche L 2012 Precursors of solvated electrons in radiobiological physics and chemistry *Chem. Rev.* **112** 5578–602
[4] Alizadeh E, Orlando T M and Sanche L 2015 Biomolecular damage induced by ionizing radiation: the direct and indirect effects of low-energy electrons on DNA *Annu. Rev. Phys. Chem.* **66** 379–98
[5] Sanche L 2003 Low-energy electron damage to DNA and its basic constituents *Phys. Scr.* **68** C108–12
[6] Caleman C, Ortiz C, Marklund E, Bultmark F, Gabrysch M, Parak F G, Hajdu J, Klintenberg M and Tîmneanu N 2009 Radiation damage in biological material: electronic properties and electron impact ionization in urea *Europhys. Lett.* **85** 18005
[7] Thürmer S, Seidel R, Faubel M, Eberhardt W, Hemminger J C, Bradforth S E and Winter B 2013 Photoelectron angular distributions from liquid water: effects of electron scattering *Phys. Rev. Lett.* **111** 1–5
[8] Suzuki Y I, Nishizawa K, Kurahashi N and Suzuki T 2014 Effective attenuation length of an electron in liquid water between 10 and 600 eV *Phys. Rev. E - Stat. Nonlinear, Soft. Matter Phys.* **90** 1–5
[9] Signorell R, Goldmann M, Yoder B L, Bodi A, Chasovskikh E, Lang L and Luckhaus D 2016 Nanofocusing, shadowing, and electron mean free path in the photoemission from aerosol droplets *Chem. Phys. Lett.* **658** 1–6
[10] Nishitani J, Yamamoto Y I, West C W, Karashima S and Suzuki T 2019 Binding energy of solvated electrons and retrieval of true UV photoelectron spectra of liquids *Sci. Adv.* **5** 1–8
[11] Signorell R 2020 Electron scattering in liquid water and amorphous ice: a striking resemblance *Phys. Rev. Lett.* **124** 205501
[12] Luckhaus D, Yamamoto Y I, Suzuki T and Signorell R 2017 Genuine binding energy of the hydrated electron *Sci. Adv.* **3** 1–6
[13] Michaud M, Wen A and Sanche L 2003 Cross sections for low-energy (1–100 eV) electron elastic and inelastic scattering in amorphous ice *Radiat. Res.* **159** 3–22
[14] Gartmann T E, Hartweg S, Ban L, Chasovskikh E, Yoder B L and Signorell R 2018 Electron scattering in large water clusters from photoelectron imaging with high harmonic radiation *Phys. Chem. Chem. Phys.* **20** 16364–71
[15] Gartmann T E, Ban L, Yoder B L, Hartweg S, Chasovskikh E and Signorell R 2019 Relaxation dynamics and genuine properties of the solvated electron in neutral water Clusters *J. Phys. Chem. Lett.* **10** 4777–82
[16] Krausz F and Ivanov M 2009 Attosecond physics *Rev. Mod. Phys.* **81** 163–234
[17] Drescher M, Hentschel M, Kienberger R, Uiberacker M, Yakovlev V, Scrinzi A, Westerwalbesloh T, Kleineberg U, Heinzmann U and Krausz F 2002 Time-resolved atomic inner-shell spectroscopy *Nature* **419** 803–7
[18] Goulielmakis E *et al* 2010 Real-time observation of valence electron motion *Nature* **466** 739–43
[19] Sansone G *et al* 2010 Electron localization following attosecond molecular photoionization *Nature* **465** 763–6
[20] Calegari F *et al* 2014 Ultrafast electron dynamics in phenylalanine initiated by attosecond pulses *Science (80-)* **346** 336–9
[21] Cavalieri A L *et al* 2007 Attosecond spectroscopy in condensed matter *Nature* **449** 1029–32

[22] Seiffert L et al 2017 Attosecond chronoscopy of electron scattering in dielectric nanoparticles Nat. Phys. 13 766–70
[23] Liu Q et al 2018 Attosecond streaking metrology with isolated nanotargets J. Opt. 20 024002
[24] Faubel M, Steiner B and Toennies J P 1997 Photoelectron spectroscopy of liquid water, some alcohols, and pure nonane in free micro jets J. Chem. Phys. 106 9013–31
[25] Corkum P B 1993 Plasma perspective on strong field multiphoton ionization Phys. Rev. Lett. 71 1994–7
[26] Even U 2015 The Even-Lavie valve as a source for high intensity supersonic beam EPJ Tech. Instrum. 2 17
[27] Eppink A T J B and Parker D H 1997 Velocity map imaging of ions and electrons using electrostatic lenses: application in photoelectron and photofragment ion imaging of molecular oxygen Rev. Sci. Instrum. 68 3477–84
[28] Yoder B L, West A H C, Schläppi B, Chasovskikh E and Signorell R 2013 A velocity map imaging photoelectron spectrometer for the study of ultrafine aerosols with a table-top VUV laser and Na-doping for particle sizing applied to dimethyl ether condensation J. Chem. Phys. 138 044202
[29] Dribinski V, Ossadtchi A, Mandelshtam V A and Reisler H 2002 Reconstruction of Abel-transformable images: the Gaussian basis-set expansion Abel transform method Rev. Sci. Instrum. 73 2634–42
[30] Barth S, Ončák M, Ulrich V, Mucke M, Lischke T, Slavíček P and Hergenhahn U 2009 Valence ionization of water clusters: from isolated molecules to bulk J. Phys. Chem. A 113 13519–27
[31] Samson J A R and Stolte W C 2002 Precision measurements of the total photoionization cross-sections of He, Ne, Ar, Kr, and Xe J. Electron Spectros. Relat. Phenom. 123 265–76
[32] Haddad G N and Samson J A R 1986 Total absorption and photoionization cross sections of water vapor between 100 and 1000 Å J. Chem. Phys. 84 6623–6
[33] Hartweg S, Yoder B L, Garcia G A, Nahon L and Signorell R 2017 Size-resolved photoelectron anisotropy of gas phase water clusters and predictions for liquid water Phys. Rev. Lett. 118 1–6
[34] Grushka E 1972 Characterization of exponentially modified gaussian peaks in chromatography Anal. Chem. 44 1733–8
[35] Öhrwall G et al 2005 The electronic structure of free water clusters probed by Auger electron spectroscopy J. Chem. Phys. 123 054310
[36] Muller H G 2002 Reconstruction of attosecond harmonic beating by interference of two-photon transitions Appl. Phys. B 74 s17–21
[37] Paul P M, Toma E S, Breger P, Mullot G, Augé F, Balcou P, Muller H G and Agostini P 2001 Observation of a train of attosecond pulses from high harmonic generation Science (80-) 292 1689–92